# Elemental and Charge State Composition in the Heliosphere

**Eberhard Möbius**

Space Science Center and Department of Physics

University of New Hampshire

**Abstract:** The heliosphere is filled with material from three samples of matter, solar material in the form of the solar wind and solar energetic particles, material from the neutral fraction of the surrounding interstellar medium, and galactic cosmic rays. In this lecture we will address the first two samples that constitute the main plasma component and evidence of their further acceleration in the heliosphere. We will review the observation techniques and some key observations, which provide information about fractionation, acceleration, and transport. For brevity we limit the discussion of the solar wind to some recurring topics that connect particularly well to the discussion of further acceleration and fractionation.

## 1 Introduction: Why Composition and Q-State?

Observation of elemental, isotopic and charge composition in heliospheric particle populations provides constraints on contributing sources and their composition. Such measurements, when taken over a wide energy range, reveal the characteristic signatures of heating, acceleration and transport of all ion species. For neutrals, ionization and filtration processes also leave their unmistakable mark. Often, these processes are highly selective in mass, charge and energy distribution. Thus, heliospheric composition measurements generate some of the most important and complex data-sets, which provide tremendous opportunities for the analysis of physical processes and cosmologically important compositional patterns.

The heliosphere is filled with and exchanges material from three different samples of matter, solar material as solar wind and a variety of energetic particles, the neutral fraction of the surrounding interstellar medium, and galactic cosmic rays (GCR). On the grand scheme these samples represent different stages of the evolution of matter in the universe and our galaxy. While primordial matter only consisted of H and He, with a very small contribution of Li and B, right after the Big Bang, heavy elements were formed in consecutive generations of stars and injected into the interstellar medium by winds of aging massive stars and supernovae. It is thought that the fraction of heavy elements continuously increases with

the age of the universe. With its formation 4.5 billion years ago, the solar system froze-in a cloud of interstellar matter at that time, with the Sun representing the lion share and most unbiased sample. The interstellar material surrounding the solar system is a contemporary sample with 4.5 billion years of additional evolution. Together with the reasonably well-understood Big Bang nucleosynthesis (Geiss and Gloeckler, 2007) the first two samples provide three composition data points over the history of the universe. GCRs contribute valuable insight into elements and isotopes, which are relatively rare, and have been mostly formed in interaction between cosmic rays and interstellar gas, such as B and Be. Therefore, a detailed abundance pattern provides key information on the evolution of matter.

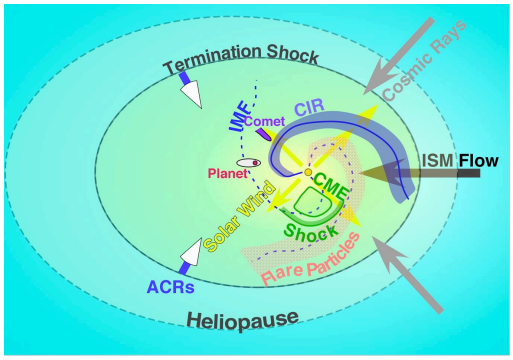


**Fig. 1:** Schematic view of the heliosphere with various particle populations, their sources, and related acceleration sites (from Möbius and Kallenbach, 2005).

Fig. 1 gives a simplified overview of sources and acceleration sites in the heliosphere. All three main sources contribute to the observed particle populations. The shading in Fig. 1 indicates how the relative importance of the solar wind (yellow) and the interstellar medium (turquoise) changes with distance from the Sun. Planets with their atmospheres, comets, asteroids, and even dust (not shown) serve as additional injectors. While these objects mostly belong to the solar system and thus inherited largely the composition of the protosolar nebula, they have undergone a variety of fractionation processes during the formation and evolution of the solar system. Only the Sun is thought to have retained mostly the original composition, since nuclear fusion is well contained in its core. A final fractionation occurs because mostly volatile elements are found in and thus released from atmospheres. On the flip side, this last step in the chain, along with the environmental conditions, which mostly determine the ionic charge state upon release, allows identification of these local sources through element and charge composition. For example, the solar wind as the extension of the 1-2 MK corona contains charge states that correspond to this temperature ($C^{5+}$, $O^{6+}$, and $Fe^{9\text{-}12+}$), while comet and planet atmospheres release almost exclusively neutral and singly ionized components.

Also shown in Fig. 1 are the most prominent acceleration sites in the heliosphere. Through solar flares, the Sun features a second channel of particle release in addition to the solar wind, which as will be seen later exhibits starkly different characteristics. Wherever the solar wind abruptly changes its velocity, it is compressed, often until a shock forms, with the consequence of effective particle acceleration. Where fast solar wind overtakes slow wind a co-rotating interaction re-

gion (CIR) forms, a pattern that rotates exactly with the Sun. Likewise, coronal mass ejections (CMEs) with their often rather high speeds lead to a similar interaction, in most cases with a leading interplanetary (IP) shock. It is reasonable to assume and indeed observed that in these interaction regions particles out of all of the present sources are accelerated, posing a challenge and at the same time providing opportunities for diagnostics. In this limited overview we restrict ourselves to particle populations produced in the inner heliosphere, thus omitting ACRs and GCRs, covered in the contribution by Saiz (***this volume***).

## 2 Key Composition Parameters

The nuclear charge number $Z$, which also equals the number of electrons, determines the element. To distinguish isotopes the mass $M$ with mass number $A$ must be obtained, where $M = A\ m_p$. Often, it is sufficient to measure A to also identify the element, because the most important isotope of each element does not have a mass counterpart in neighboring elements.

The ionic charge state $Q$ is determined by how many electrons an atom has lost. $Q$ can range from 0 to $Z$ and thus should be clearly distinguished from the latter. Generally, higher temperatures lead to the extraction of more electrons, because higher energy is needed to eject additional electrons from inner shells. For equilibrium conditions the relation between temperature and $Q$ has been compiled for a number of elements (Mazzotta et al., 1998, and references therein). A combination of ionic charge $Q$ and mass $A$ along with their actual energy $E$ usually determines the acceleration and transport of different species.

In summary, the combination of $A$ and/or $Z$, $Q$, and $E$ is needed to carry out a successful composition measurement. Often either $A$ or $Z$ is sufficient, and for many studies $Q$ is not needed. Still, to obtain composition and energy, a combination of two or more measurement techniques is needed. In this paper we will present a few such combinations that have been implemented in space-born instruments, followed by observations of the solar wind and energetic particles.

## 3 Techniques for Solar Wind and Suprathermals

Detailed composition measurements in the solar wind started with the deployment of thin metal foil sails on the moon during the Apollo missions and their return to Earth. After solar wind had been implanted over several hours or days on the moon, the captured content was analyzed in the laboratory (Geiss et al., 1972), leading to the first average element and isotope abundances in the solar wind. However, this method does not allow tracking of temporal changes, long term monitoring, and has other limitations, which called for in-situ methods.

*- Electrostatic Analyzers*

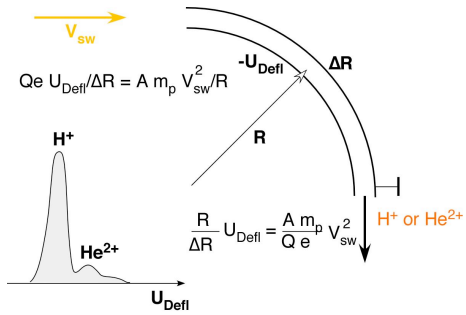


**Fig. 2:** Schematic view of solar wind observations with an electrostatic analyzer.

Since the beginning of the space age solar wind observations are being made using electrostatic analyzers in the form of Faraday Cups (Vasyliunas, 1971) and hemi-spherical analyzers (Gosling et al., 1978) that utilize retarding potentials and electrostatic deflection, respectively, for energy selection. Fig. 2 shows functional principles for the example of a schematic solar wind spectrum shown here as a function of deflection voltage ($U_{\mathrm{Defl}}$) for a hemispherical analyzer. It demonstrates how such an analyzer provides species identification in combination with the defined flow speed of the solar wind, which translates into a common energy per mass $E/A$ for all species. A hemispherical analyzer consists of two concentric hemispheres with radius $R$ and separation $\Delta R$, of which the inner one usually is biased with a negative deflection voltage. For ions that pass the analyzer on a central trajectory the centripetal force $Am_p v_o^2/R$ balances the electrostatic force $QeU_{\mathrm{Defl}}/\Delta R$. For a given $U_{\mathrm{Defl}}$ ions of a certain energy per charge $E/Q$ pass through the analyzer. In our example the speed of the particles is the solar wind speed, i.e. $v_o = v_{sw}$. Combining $E/Q$ with the common $E/A$, the analyzer separates species with distinctly different $A/Q$, as shown in the lower left of Fig. 2 for $H^+$ and $He^{2+}$. The separation capability is determined by the width of the solar wind velocity distribution $\Delta v/v_o$ and the analyzer resolution $\Delta(E/Q)/(E/Q)$. With $\Delta v = v_{th}$ (solar wind thermal speed) and $\Delta(E/A)/(E/A) \approx 2\Delta v/v_o$, the combined $A/Q$ resolution of the analyzer becomes:

$$\frac{\Delta(A/Q)}{A/Q} = \sqrt{\frac{4v_{th}^2}{v_o^2} + \frac{\Delta(E/Q)^2}{(E/Q)^2}} \qquad (2.1)$$

For a typical analyzer resolution of 3-10% species identification depends heavily on the solar wind being cold. $H^+$ and $He^{2+}$ typically can be resolved, but it becomes much more challenging, if not impossible, to separate $O^{6+}$ and $Fe^{10+}$ from $He^{2+}$ and each other. Moreover, this method is restricted to the bulk solar wind.

- *Time-of-flight Spectrometers*

Progress towards mass resolution independent of the solar wind distribution was made with magnetic mass spectrometers and most recently with time-of-flight spectrometers. Figure 3 shows a schematic cross-section and the governing relations for a time-of-flight (TOF) mass spectrometer.

After passing an electrostatic analyzer, which selects the ions for $E/Q$, they pass a thin ($\approx$1-3 $\mu$g/cm$^2$) carbon foil, from where they move on to a solid-state

detector (SSD) (or a micro-channel plate (MCP)) for a path length $s$. To achieve a reasonably good resolution after energy loss in the foil, the energy of incoming ions is boosted by post-acceleration with $U_{Acc} = 15 - 25$ kV, resulting in

$$E_A/Q = eU_{Acc} + E/Q. \qquad (2.2)$$

The ions release secondary electrons from the C-foil and the surface of the SSD, which - by means of appropriate electrostatic potentials - are accelerated and steered to MCPs for detection as start and stop signals to record the TOF $\tau$. The energy per mass of the incoming ion is then

$$\frac{a_1 E_A}{A m_p} = \frac{s^2}{2\tau^2} \qquad (2.3)$$

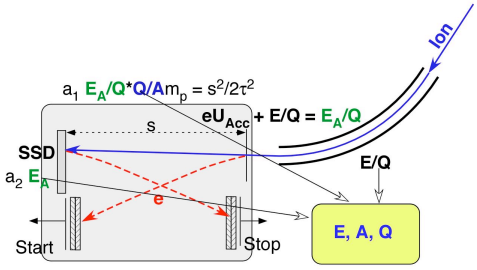


**Fig. 3:** Schematic cross-section and functional diagram of a time-of-flight mass spectrometer.

where $a_1 \leq 1$ is the fraction of the ion energy after passing the foil. Combining 2.2 and 2.3 yields $A/Q$. The SSD returns the residual ion energy $a_2\, E_A$, where $a_2$ is the fraction of the energy that is actually detected. Both $a_1$ and $a_2$ vary with energy and species and are determined in calibration at an ion accelerator. Including the residual energy in the analysis yields $E$, $A$, and $Q$ of the incoming ion separately. An overview of TOF spectrometers may be found in Wüest (1998) and Young (2002).

*- High-Resolution Time-of-flight Spectrometers*

Linear TOF spectrometers as described above are limited in their resolution by the energy and angle spread after energy and angular straggling due to the interaction with the C-foil. These limitations can be circumvented if the ions traverse a ballistic trajectory in a retarding electric field whose strength increases linearly with distance from the plane in which the entrance foil and the stop detector are located (Fig. 4). Because of the linearly increasing electric field $E(y) = k \cdot y$ the TOF $\tau$ is half the period of a harmonic oscillator for an ion with mass per charge $A/Q$.

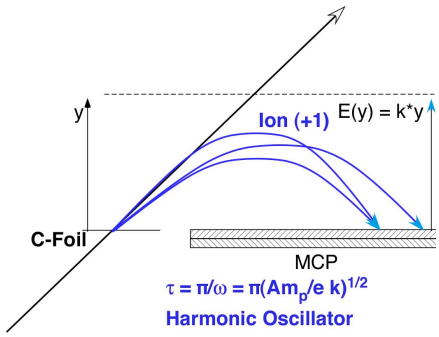


**Fig. 4:** Schematic cross-sectional view of a high-resolution TOF spectrometer, including ballistic trajectories of ions in the retarding electric field $E(y)$. The time-of-flight $\tau$ equals half the period of a harmonic oscillator.

$$\tau = \frac{\pi}{\omega} = \pi\sqrt{\frac{Am_p}{ek}} \tag{2.4}$$

Relation 2.4 is for singly charged ions because the majority of ions will either be neutral or singly charged after passage of the C-foil with energies that range from 1 to 30 keV/e, requiring a retarding potential of ≈20 kV for 45° trajectories. Neutral particles leave the TOF on a straight line, while singly charged ions reach the stop detector. Neither initial energy nor incoming angle matter for the resulting TOF, which solely depends on $A/Q$, or on $A$ for $Q = 1$ (Wüest, 1998, and references therein).

# 3 Key Composition Observations in the Solar Wind

The solar wind exhibits large variations in its abundances of heavy ions on time scales of hours or even down to minutes that can amount up to almost a factor of ten. Also the charge states of the ions vary along with the abundance variations. Usually, charge states are expressed in terms of their freeze-in temperature, i.e. the temperature for which the observed charge states occur in equilibrium state. Because the solar wind expands rapidly as it emerges from the corona its density falls and collisions become so rare that the original charge states are frozen in during the expansion of the solar wind (for a review see Bochsler, 2007).

*- The FIP Effect*

Systematic studies of solar wind abundances with Ulysses SWICS have shown that low freeze-in temperatures and high abundances of, for example Si and Fe compared with O, are associated with high-speed solar wind and vice versa (von Steiger et al., 2000; Figure 5). In particular, the abundance ratios show much sharper boundaries between the solar wind types than speed. Therefore, the abundances are often taken as a better indicator for fast and slow solar wind.

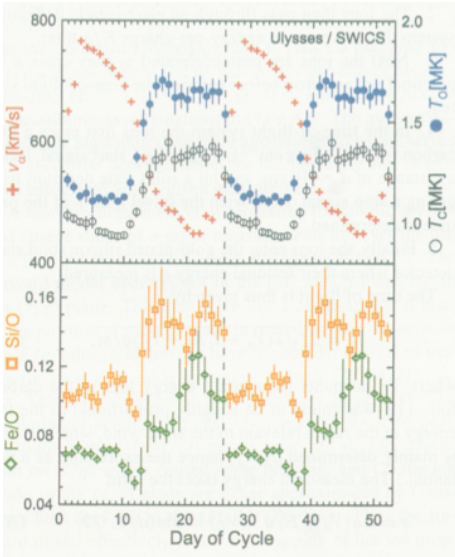


**Fig. 5**: Superposed epoch analysis of Ulysses SWICS solar wind composition data for fast to slow solar wind transitions (von Steiger et al., 2000). Overlaid are solar wind speed, C and O temperatures (top), Si/O and Fe/O (bottom).

When organizing the solar wind abundance ratios according to the first ionization potential (FIP), it turns out that generally the elements with values below the FIP of H (13.6 eV) are enhanced over

those with FIP values at or above that of H, when compared with photospheric abundances. This is interpreted as a competition of magnetic lifting out of the photosphere and gravitational settling.

*- Isotope Fractionation*

Measuring the isotopic ratios of refractory elements in the solar wind has not turned up a significant fractionation relative to the ratios in the closest proxies of the protosolar nebula, meteorites and Jupiter. A weak trend in the ratio with solar wind speed is found, consistent with the expected effects of Coulomb drag, but so far these results are not statistically significant yet (Kallenbach et al., 1998, and review by Bochsler, 2007). However, occasionally a substantial fractionation of $^3$He is observed in CME ejecta (c.f. review by Zurbuchen and Richardson, 2006).

*- Implantation of Singly Charged Pickup Ions*

The heliosphere is also populated with a number of neutral gas sources. Ionization by solar UV photons, charge exchange with solar wind ions and electron impact turns neutrals into ions. These newborn ions are picked up by the interplanetary magnetic and convectional electric fields, forced to gyrate about the magnetic field, and consequently swept radially outward with the solar wind. Through pitch-angle diffusion and adiabatic cooling of the velocity distribution in the radially expanding solar wind these pickup ions typically fill a sphere in velocity space with radius equal to the solar wind speed around the solar wind velocity (see review by Szegö et al. (2000).

The most extended source of such pickup ions is the neutral interstellar gas, which penetrates the entire heliosphere. $He^+$ ions were detected first (Möbius et al., 1985), followed by $H^+$ and heavy ions (see review by Gloeckler & Geiss, 2001). While interstellar ions become more important at larger distances from the Sun due to their continuous implantation into the solar wind, the so-called inner source, thought to originate from interplanetary dust, is concentrated close to the Sun (for a review see Allegrini et al., 2005). In addition, to these extended sources, localized pickup ions have been found in the vicinity of comets or planetary atmospheres. Common distinctions of pickup ions from the solar wind are their broad velocity distributions and the fact that they are singly charged.

# 4 Techniques for Composition of Energetic Ions

To expand composition measurements into the suprathermal and medium energy range up to ≈1 MeV/nuc the same measurement techniques as presented in section 2 for solar wind energies can be used. In fact, the task is simplified for somewhat higher energies because no post-acceleration with its high voltage challenges is needed. However, with increasing energy the TOF decreases for a given path length, which, with limited timing resolution, determines the upper energy limit for TOF sensors (≈1 MeV/nuc).

*- ΔE – E Telescopes*

Above a few 100 keV/nuc, overlapping with the TOF technique, energy loss in matter, which has been limiting TOF resolution through energy straggling in the C-foil, can in turn be used as a tool. The most important interaction of ions while penetrating matter consists of Coulomb collisions with electrons. For individual collisions at non-relativistic energies the momentum change $\Delta p_e$ of the ion is:

$$\Delta p_e \approx \overline{F} \bullet \overline{\Delta t} = \frac{Z^* e^2}{4\pi\varepsilon_o b^2} \bullet \frac{2b}{v} = \frac{2 \bullet Z^* e^2}{4\pi\varepsilon_o b v} \qquad (4.1)$$

$F$ is the Coulomb force and $Z^*$ is the effective charge of the penetrating ion, which is equal to $Z$ for energies >1 MeV/nuc. For illustration purposes the total interaction has been approximated by integration only along a path of $2b$ ($b$ being the impact parameter, i.e. the closest distance between the collision partners). The corresponding energy loss $\Delta E_e$ follows as:

$$\Delta E_e = \frac{\Delta p^2}{2m_e} = \frac{2 Z^{*2} e^4}{(4\pi\varepsilon_o)^2 b^2 v^2 m_e} \qquad (4.2)$$

The total energy loss $\Delta E$ is the sum over all collisions with different impact parameters $b$ for the electron density and thickness $\Delta L$ of the detector. Carrying only the relevant proportionalities $\Delta E$ is:

$$\Delta E \sim Z^{*2} / v^2 \sim Z^{*2} A / E \qquad (4.3)$$

From $\Delta E$ and $E$ the nuclear charge $Z$ and mass number $A$ can be determined. Fig. 9 shows an arrangement of a thin detector for $\Delta E$ determination and a thick detector to stop the ion and determine $E$. For high energies both can be SSDs of different thickness. For energies below a few MeV/nuc the thin detector has to be a gas detector, which features a much lower matter density than solids. In a gas counter the penetrating ions ionize a certain number of atoms, and the resulting electrons are collected as a charge signal, which is proportional to the energy loss $\Delta E$, hence proportional counter. For a description of these techniques see the book by Ahmed (2007).

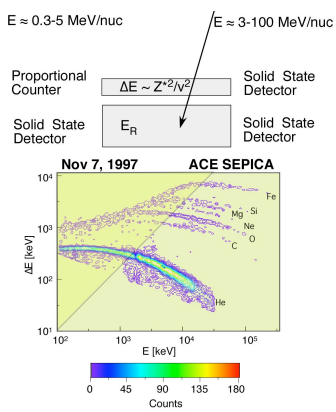


**Fig. 6:** Top: Schematic view of a $\Delta E$ - $E$ particle telescope with combinations for different energy ranges. Bottom: $\Delta E$ – $E$ diagram for an SEP event. Tracks for individual elements are clearly separated except for energies below ≈ 0.3 MeV/nuc.

The lower portion of Fig. 6 shows a $\Delta E$ - $E$ representation of an SEP event taken with

ACE SEPICA (Möbius et al., 1998). Mostly individual tracks are clearly identifiable for each element. At the highest energies they fall off as $1/E$ (see 4.3). Below ≈1 MeV/nuc the tracks of heavier ions turn over and merge with other species at the low energy end (indicated by the yellow triangle), reflecting pickup of electrons in the detector material, thus reducing $Z^*$ to $Z^* < Z$.

*- Ionic Charge State Measurement at High Energies*

To also determine the ionic charge state $Q$ requires the addition of a third measurement. At moderately high energies (≤3 MeV/Q) this can be achieved with electrostatic deflection, but not with spherical analyzers. Firstly, for MeV energies this would lead to a combination of rather large radii and extremely high deflection voltages. Secondly, the necessary stepping through energy makes the effective geometric factor too low for the steep energy spectra. Therefore, mechanical collimator with subsequent deflection and position measurement is used (ACE SEPICA example in Fig. 7, Möbius et al., 1998).

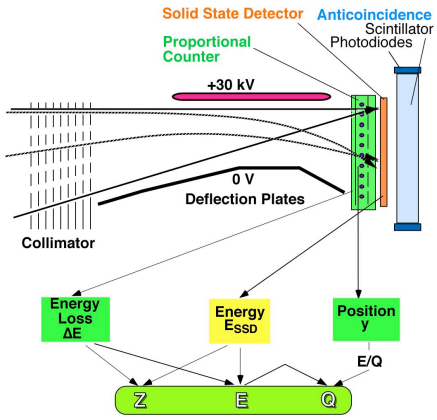


**Fig. 7:** Schematic cross-sectional view of the ACE SEPICA sensor (Möbius et al, 1998) with its functional principles.

Above a few MeV/Q electrostatic deflection becomes too small in any reasonably sized sensor. To extend charge state measurements the assistance of the Earth's magnetic field has been enlisted. Saiz and Taka? (***this volume***) describe how penetrating cosmic ray fluxes at low Earth orbit satellites and on the ground depend on magnetic rigidity $R$ and the location within the Earth's magnetic field.

$$R = \frac{pc}{Qe} = \frac{c\sqrt{2Am_pE}}{Qe} \tag{4.4}$$

Close to the poles the cut-off rigidity depends distinctly on the magnetic latitude. Thus Q can be determined if $A$ and $E$ are measured with a sensor as described above. The cut-off method is being employed successfully on SAMPEX for 0.5 to several 100 MeV/nuc (Baker et al., 1993, and references therein).

# 5 Key Observations with Energetic Particles

The general behavior of solar energetic particles (SEPs) is discussed by Saiz? (***this volume***) and shall not be repeated here. We will rather concentrate on com-

positional aspects in heliospheric energetic particles. It should suffice to note that SEPs are usually subdivided into two groups. Large gradual events typically last for days, are accompanied by CMEs, and averaged over many events show abundances and ionic charge states of the corona. Mostly small, impulsive events, only last for a few hours, are associated with compact flares, and show substantial enhancements in ions heavier than O and in $^3$He over $^4$He, hence $^3$He-rich events. For an overview the reader is referred to the paper by Reames (1999) and references therein.

### 5.1 Elemental and Isotopic Composition

*- Gradual SEPs*

In several extended surveys it has been found that, averaged over a number of events, gradual SEPs show abundances and charge states that reflect coronal values. However, they also exhibit substantial event-to-event variations, which range from significant depletions to enhancements, for example, in Fe (Fe-poor and Fe-rich) (Reames 1999). Usually, the observed enhancements/depletions exhibit a trend in Q/A indicating Q/A dependent selection processes that may be attributed to acceleration, escape, and/or transport of the ions in these events.

Because on average gradual SEPs reflect the composition of the corona they also bear the imprint of the FIP effect as found in coronal and solar wind composition. While also the strength of the FIP effect varies from event to event, it is typically closer to the more pronounced value observed in the slow solar wind (Reames, 1999). This may indicate the source material for the acceleration originates from the closed field region where also the slow wind stems from. However, it should be noted that the observed variations in the FIP effect make it impossible at the moment to pin down exactly the source of the gradual SEPs.

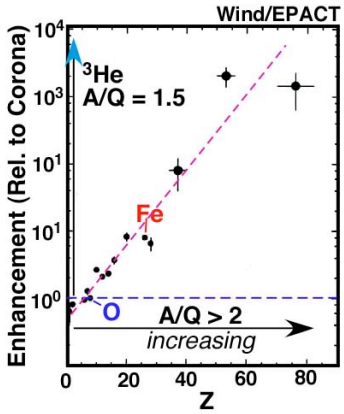


**Fig. 8**: Abundances in impulsive events as compared with the corona, organized in A/Q (adapted from Reames et al., 2001).

*- Impulsive SEPs*

The event-to-event variations in gradual SEP composition are usually only substantial for ions with starkly different A/Q values and they vary in both directions. Conversely, abundances in impulsive SEPs can also be substantially enhanced for neighboring elements, and heavy ions are always enhanced over light ions. For example, Ne is substantially enhanced over O, up to a factor of 10 in some events. Again, the enhancement of heavy ions can be organized in terms of A/Q, assuming ionic charge states that resemble a 3-5 million K corona (Reames, 1999). As can be seen in Fig. 8, heavy ion abundances

increase approximately exponentially in A/Q, with ultra-heavy elements (Z = 60-80) exceeding a factor of 1000 (Reames, 2000; Mason et al., 2004). However, the substantial enhancement of $^3$He in these events does not fit into this trend is, because A/Q = 1.5 goes into the opposite direction. Compared to the natural $^3$He/$^4$He ratio of $5 \cdot 10^{-4}$ enhancements up to $10^4$ have been observed with $^3$He/$^4$He ratios exceeding 1.

Proposed models invoke selective heating and acceleration through resonant wave-particle interaction. Suggested are ion-acoustic turbulence, electrostatic ion cyclotron waves, electromagnetic ion cyclotron waves, and cascading Alfvénic turbulence (For an overview see the reviews by Reames, 1999, and Wiedenbeck et al., 2008). While any of these models explain some of the observations, mostly qualitatively, none of them provides a complete quantitative explanation. The recently observed strong enhancement of ultra-heavy ions has dealt even the most successful models a significant blow. It should be emphasized though that all of them so far rely on differences in A/Q for any enhancement. Therefore, ionic charge states for all species are very important to assess any explanatory model.

### 5.2 Ionic Charge States

First charge state observations, averaged over all impulsive events of an entire year returned a puzzling result. The mean charge of Fe was found to be typically $Q \approx 20$, and all species up to Si appeared to be fully stripped, i.e $Q = Z$ (Klecker et al., 2007). With A/Q = 2 under fully stripped conditions there is no leverage for A/Q dependent fractionation. With ACE SEPICA resolution and collection power have been improved substantially so that individual impulsive event observations, even separated by energy, have become available.

*- Energy dependence of Q*

Early ionic charge state observations for both types of SEPs showed no energy dependence and supported the conclusion that charge states were frozen-in based on the temperature of the source plasma. However, observations in an extended energy range with SAMPEX showed a charge state increase above a few MeV/nuc. The first major SEP event observed with ACE even showed an increase in the Fe charge state of $\Delta Q > 4$ at 0.2 - 0.5 MeV/nuc, which was also seen simultaneously with SAMPEX, followed by several similar cases. Such a strong energy dependence of the charge state requires stripping of the energetic ions in ambient material as an explanation (review by Klecker et al., 2007).

Because the most important ionization process in plasmas involves electron impact each element is effectively ionized up to the point when the necessary ionization potential exceeds the electron thermal energy. When energetic ions pass through the plasma at a speed that exceeds the thermal electron speed the ion energy starts to play a role in the formation of the charge state. At plasma temperatures of $10^6$ K ($1\text{-}2 \cdot 10^6$ K are typical for the corona) ion speeds at $\approx$0.25 MeV/nuc are comparable to the electron thermal speed, i.e. the energy where the charge

state increase indeed starts some of the events. However, to leave a noticeable effect in the charge state of the energetic ions enough collisions must occur between the source and the observer. The necessary condition is either expressed as a column density $n \cdot l$ (with plasma density $n$ and path length of traversal $l$) or a product $n\tau$ with total travel and acceleration time $\tau$. For typical values of the ionizing cross sections of $10^{-16}$ cm$^{-2}$ the two conditions read $n \cdot l \geq 10^{19}$ cm$^{-2}$ and $n \cdot \tau \geq 10^{10}$ cm$^{-3}$s.

These new findings suggested a strong energy dependence also for impulsive SEP events, which whose source is in the solar atmosphere. This would be consistent with partial ionization at low energies where the observed strong ion fractionation supposedly starts and full ionization at high energies. Indeed such behavior was found for impulsive events in observations with ACE SEPICA and at even lower energies with SOHO STOF as shown in Fig. 9 together with modeling that assumes energetic ions achieving equilibrium charge states for each energy after emerging from plasmas with two different temperatures (Klecker et al., 2007). To achieve quantitative agreement finite residence times in the plasma and adiabatic deceleration of the ions from the source to 1 AU must be included. The low energy observations constrain the source temperature to ≈ 1.2-1.8 · $10^6$ K. The observed energy dependence requires acceleration of the ions in the lower corona – for all impulsive and certain gradual SEP events that exhibit a similar behavior.

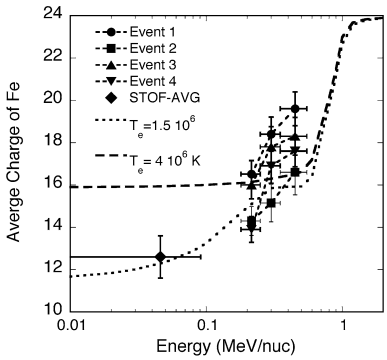


**Fig. 9**: Fe charge states in 4 impulsive SEP events and equilibrium models with stripping (Klecker et al., 2007).

### 5.3 Sources and Fractionation in Interplanetary Space

While SEPs in impulsive events have been traced to acceleration at the flare site, for CME related events shock acceleration of ambient material is invoked. A subset of these events shows ongoing particle acceleration even at 1 AU. As it turns out CME driven shocks are not the only ones accelerating particles in interplanetary space. The succession of slow and fast solar wind leads to compression regions, which rotate with the Sun, hence co-rotating interaction regions (CIR). Compression regions and the shocks that usually form at ≥1 AU are known as formidable particle accelerators from localized energetic particle flux increases. For overviews see Reames (1999) and Möbius & Kallenbach (2005).

Given the location of this acceleration, the solar wind has been implicated as a source for the resulting energetic particles. However, the observation of prominent contributions of $^3$He and heavy ions with the abundance pattern of impulsive SEP events at interplanetary shocks and of He$^+$ in CIRs and at shocks support conclu-

sion that source populations with substantially wider velocity distributions than the relatively cold solar wind are injected and accelerated much more effectively in interplanetary space. The abundance of $^3$He and heavy ions at shocks correlates well with the abundance pattern measured before the shock arrival, while there is no correlation with solar wind abundance. $He^+$ that stems from interstellar pick up ions and is present as a suprathermal distribution between $v = 0$ and $2v_{sw}$ shows up in $He^+/He^{2+}$ ratios that exceed the abundance of pickup ions relative to the solar wind by factors of 100-200. Both findings clearly support that suprathermal particle populations are strongly favored in the injection process into acceleration as argued by Möbius and Kallenbach (2005) in their review of recent observations.

# 6. Summary and Conclusions

Instrumentation that provides elemental, isotopic, and ionic charge state composition has become available with impressive resolution and collection power for an extended energy range, which covers three samples of cosmic matter in the heliosphere: the Sun, from solar wind and SEPs, the local interstellar cloud, from pickup ions and anomalous cosmic rays, and finally galactic cosmic rays. When it comes to the question, how well these observations reveal the composition of these sources we discover a number of processes that alter the original abundance ratios to what is observed. In turn, composition measurements have helped tremendously to understand these fractionation processes. Each step in their understanding and more complete samples will better constrain the source composition.

Starting at the original sources, abundances may be biased in the transition from neutral atoms to ions, through differences in the first ionization potential (FIP) between species. In addition to gravitation and heat, charged particles can also be affected by electric and magnetic fields, which may lead to preferential escape from the source regions. For subsequent fractionation steps the mass per charge ratio $A/Q$ appears to be the ruling parameter, which is determined once element, isotope, and charge state are known. However, quite often the ionic charge state can change substantially in the interaction with intervening matter. As a result, the observed charge states in these populations vary with energy, thus carrying the imprint of the entire interaction history. As a consequence, charge states must be measured over the entire energy range of interest, along with elemental composition, to pin the observations unquestionably to fractionation models.

In summary, composition measurements have been and are still invaluable for the determination of source distributions and all the following physical processes that alter abundances in the course of injection, acceleration, escape, and transport.

*Acknowledgments*: Work on this manuscript was partially supported under NASA Grants NAG 5-12929 and NNG06GD55G.

# 7. References


Ahmed, S. N., Physics and engineering of radiation detection, Academic Press, Boston, 2007.

Allegrini, F., N. A. Schwadron, D. J. McComas, G. Gloeckler, and J. Geiss, Stability of the inner source pickup ions over the solar cycle, *J. Geophys. Res.*, **110**, doi:10.1029/2004JA010847. 2005.

Baker, D.N., et al., An Overview of the Solar, Anomalous, and Magnetospheric Particle Explorer (SAMPEX) Mission. *IEEE Trans. Geosci. & Remote Sens.*, 1993. 31: p. 531-541.

Bochsler, P., Minor Ions in the Solar Wind, *A & A Rev.*, **14**, 1 – 40, 2007.

Geiss, J., Buehler, F., Cerutti, H., Eberhardt, P., Solar-Wind Composition Experiment, NASA SP-289, 25-122, 1972.

Geiss, J., and G. Gloeckler, Linking Primordial to Solar and Galactic Composition, *Space Sci. Rev.*, 130, 5-26, 2007.

Gloeckler, G., and J. Geiss, Heliospheric and Interstellar Phenomena Deduced From Pickup ion Observations, *Space Sci. Rev.*, 97, 169-181, 2001.

Gosling, J. T., J.R. Asbridge, S.J. Bame, and W.C. Feldman, *Rev. Sci. Instrum.,* **49**, 1260, 1978.

Kallenbach R, et al.., (1998) Fractionation of Si, Ne, and Mg Isotopes in the Solar Wind as Measured by SOHO/CELIAS/MTOF, *Space Sci. Rev.*, **85**, 357-370, 1998.

Klecker, B., E. Möbius, and M. Popecki, Ionic Charge States of Solar Energetic Particles: A Clue to the Source, *Space Sci. Rev.,* 130, 273-282, 2007.

Mason, G. M., et al., Abundances of Heavy and Ultraheavy Ions in $^3$He-rich Solar Flares, *Astrophys. J.*, 606, 555-564, 2004.

Mazzotta, P., Mazzitelli, G., Colafrancesco, S., and Vittorio, N., *Astron. Astrophys. Suppl.*, 133, 403, 1998.

Möbius, E., et al., Direct observation of $He^+$ pick-up ions of interstellar origin in the solar wind, *Nature*, 318, 426 - 429, 1985.

Möbius, E., et al., *Space Sci. Rev.*, 86, 447, 1998.

Möbius, E., R. Kallenbach, Acceleration in the Heliosphere, The Heliosphere and Beyond/10 Years of ISSI, J. Geiss and B. Hultqvist eds., ISSI-SR003, 165, 2005.

Reames, D.V., Particle acceleration at the Sun and in the heliosphere, *Space Sci. Rev.*, 90, 413-491, 1999.

Reames, D. V., Abundances of Trans-Iron Elements in Solar Energetic Particle Events, *Astrophys. J.*, 540, L111-L114, 2000.

Saiz, A., (***this volume***)

Sako, T., (***this volume***)

Szegö, K., et al., Physics of Mass Loaded Plasmas, *Space Sci. Rev.*, 94, 429, 2000.

Vasyliunas, V. M., Deep space plasma measurements, in: *Methods of Experimental Physics*, R. H. Lovbergs, ed., 9, 49-88, 1971.

von Steiger, R., et al., Composition of quasi-stationary solar wind flows from Ulysses/Solar Wind Ion Composition Spectrometer, *J. Geophys. Res.*, 105, 27217-27238, 2000.

Wiedenbeck, M., et al., $^3$He-Rich Solar Energetic Particle Events and their Association with Activity at the Sun, *Space Sci. Rev.*, in prep., 2008. (***may have to be omitted if not in press!!***)

Wüest, M., Time-of-Flight Ion Composition Measurement Technique for Space Plasmas, in: *Measurement Techniques in Space Plasmas – Particles*, R. F. Pfaff, J. E. Borovsky and D. T. Young eds., *Geophys. Monograph* 102, p. 141, AGU, 1998.

Young, D. T., Mass Spectrometry for Planetary Science, in: *Atmospheres in the Solar System: Comparative Aeronomy*. M. Mendillo, A. Nagy, and J.H. Waite eds.. *Geophys. Monograph* 130, p. 353, AGU, 2002.

Zurbuchen, T.H., and I.G. Richardson, In-Situ Solar Wind and Magnetic Field Signatures of Interplanetary Coronal Mass Ejections, *Space Sci. Rev.,* **123**, 23 – 41, 2006.